

# Investigation on the Therapeutic Mechanism of Danbie Capsules for Endometriosis: A Network Pharmacology Approach

Lina Zhang<sup>1-3,\*</sup>, Ruibin Wu<sup>2,3,\*</sup>, Tenghui Ma<sup>2,3</sup>, Wenwen Fu<sup>2,3</sup>, Jiamin Chen<sup>2,3</sup>, Lingling Li<sup>2,3</sup>, Qing He<sup>2,3</sup> 

<sup>1</sup>The First Clinical Medical College, Guangzhou University of Chinese Medicine, Guangzhou, 510080, People's Republic of China; <sup>2</sup>Department of Clinical Nutrition and Microbiome; Biomedical Innovation Center, The Sixth Affiliated Hospital, Sun Yat-sen University, Guangzhou, 510655, People's Republic of China; <sup>3</sup>Key Laboratory of Human Microbiome and Chronic Diseases (Sun Yat-sen University), Ministry of Education, Guangzhou, People's Republic of China

\*These authors contributed equally to this work

Correspondence: Qing He, Email heqing5@mail.sysu.edu.cn

**Objective:** To explore the active substances and targets of Danbie Capsules in Endometriosis therapy.

**Methods:** This study was conducted through TCMS and published literature screened and obtained 183 active substances of Danbie Capsules, combined and intersected with Endometriosis target genes collected and screened in the GEO database, obtained 24 target genes for Endometriosis treatment, and mapped the target network map of Danbie Capsules active substances against Endometriosis. The network was analyzed with the aid of Cytoscape version 3.9.1. With the aid of the platform of the STRING data analysis, PPI network analysis was conducted on 24 anti-Endometriosis targets of the Danbie Capsules.

**Results:** The research results obtained three critical active substances, namely, Quercetin,  $\beta$ -sitosterol, and Luteolin. Seven critical targets were identified, and two representative genes (TP53 and AKT1) have been verified in Macromolecular docking and immunohistochemical verification.

**Conclusion:** The active substances of Danbie Capsules in the treatment of Endometriosis are Quercetin,  $\beta$ -sitosterol and Luteolin, and the main targets are TP53 and AKT1.

**Keywords:** danbie capsules, endometriosis, network pharmacology

## Background

Endometriosis, as a chronic inflammatory disorder characterized by the ectopic localization of endometrial tissue outside the uterine cavity, can result in pelvic pain and infertility. This condition represents a substantial public health burden due to its profound influence on the quality of life of the affected women.<sup>1</sup> Endometriosis is recognized as one of the prevalent benign gynecological proliferative disorders among premenopausal women, with an estimated prevalence of 10–15% among women of childbearing potential. The exact biological mechanisms underlying endometriosis remain not fully understood. Despite being a prevalent disorder, the pathophysiology of endometriosis remains elusive. Furthermore, recent studies have suggested a lack of association between the severity of the disease and the manifestation of symptoms. Currently, there is a lack of widely used blood-based diagnostic tests specifically designed for endometriosis. Moreover, no universally effective treatment approach can guarantee the complete resolution of the condition.

Endometriosis belongs to the “sticking mass” category in Traditional Chinese medicine. Traditional Chinese medicine believes that this disease is caused by the stagnation of qi and blood stasis and the stagnation of blood stasis. Danbie Capsules are composed of 12 drugs, including Herba Scutellariae Barbatae, Radix Notoginseng, Rhizoma Sparganii, Rhizoma Curcumae, Semen Persicae, Radix Angelicae Sinensis, Turtle Carapace, Seaweed, Largehead Atractylodes Rhizome,

Cortex Eucommiae, Herba Scutellariae Barbatae, and Ramulus Cinnamomi. The combination of various drugs aims to promote blood circulation, dissipate blood stasis, and soften and disperse nodules.

Hu Sisi et al found that Danbie Capsules can reduce the concentration of PGE2 and TNF- $\alpha$  in the blood of EMs rats, which may be one of the effective mechanisms for its treatment of endometriosis.<sup>2</sup> Liu Zhenming et al research showed that Danbie Capsules have a certain therapeutic effect on Endometriosis. According to the influence on cytokines and grafts, the Active substance in the prescription is separated, and its action target and specific action mechanism are studied according to the active substance.<sup>3</sup> Zhang Chunhong et al found that Danbie Capsules can exhibit inhibitory effects on the proliferation of ectopic endometrial tissue. This effect was attributed to the reduction in the levels of prostaglandin E2 (PGE-2) and tumor necrosis factor (TNF) in both the serum and peritoneal fluid of the experimental rat models. The anti-inflammation, analgesia, improvement of blood rheology and microcirculation, and other functions are very crucial in the treatment course of Endometriosis. It embodies the distinctive principles and features of traditional Chinese medicine (TCM), which is characterized by multiple components and multiple action steps.<sup>4</sup> But its precise mechanism of action is still elusive.

Network pharmacology, an interdisciplinary field integrating pharmacology, bioinformatics, and other relevant disciplines, employs system network analysis to unravel the intricate mechanisms underlying the therapeutic effects of multi-component and multi-target drug treatments. By constructing comprehensive networks encompassing “disease-phenotype-gene-drug” interactions, this approach provides insights into gene distribution patterns, molecular functions, and signaling pathways. Notably, network pharmacology presents a particularly valuable methodology for investigating the complex mechanisms of action exhibited by TCM compounds.<sup>5</sup>

## Data and Methods

### Collection and Target Screening of the Active Substances in Danbie Capsules

After retrieving the Traditional Chinese Medicine Systems Pharmacology Database and Analysis Platform (TCMSP) (<https://tcmsp.com/index.php>) and referencing relevant kinds of literature, we got information on the active substances and their corresponding target proteins in various TCMs present in Danbie Capsules. The search was performed with the following key words: “Largehead Atractylodes Rhizome”, “Scutellaria Barbata”, “Radix Angelicae Sinensis”, “Herba Scutellariae Barbatae”, “Cortex Eucommiae”, “Radix Curcumae”, “Ramulus Cinnamomi”, “Seaweed”, “Rhizoma Sparganii”, “Radix Notoginseng”, “Semen Persicae”, and “Turtle Carapace”; screening criteria were set as oral bioavailability (OB)  $\geq 30\%$  and drug likeness (DL)  $\geq 0.18$ . For the TCM “Turtle Carapace”, due to no information available in the TCMSP database, the active substances were determined by referring to published literature,<sup>6</sup> and the corresponding target protein was obtained from the Drug Bank database using the chemical name as the search term.

By using the STRING database to uniformly change and save the form of the target protein into the target gene, we obtained the target gene set of active substances in Danbie Capsules.

### Acquisition of Differential Genes in Endometriosis

Gene sample series for patients with endometriosis and healthy individuals were obtained from the GSE25628 dataset, retrieved from the GEO database (<https://www.NCBI.NLM.NIH.gov/GEO/>). The R4.2.1 software installed R packages containing “GEOquery”, “limma”, “ggplot2” and “ComplexHeatmap”. We downloaded GSE25628 from the GEO database by using the GEOquery package, standardized the data by using the normalize Between Arrays function, and performed difference analysis between the two groups by using the limma package. Then Log<sub>2</sub> (logFC) transformation was applied, and samples with a P-value  $< 0.005$  and  $|\log_2(\text{FC})| > 1$  were considered genes that are statistically significantly differentially expressed. The gene volcano map of these samples was plotted, and the top 20 genes exhibiting the most significant upregulation or downregulation were selected to draw a heatmap.

### Determination of Targets and Network Construction of Danbie Capsules in Endometriosis Treatment

The R4.2.1 software was utilized to map the action targets of Danbie Capsules with the endometriosis-related targets using and obtaining the potential action targets (intersection targets) of Danbie Capsules in endometriosis treatment and

drawing a Venn diagram. The active substances of Danbie Capsules and their corresponding targets were imported into Cytoscape version 3.9.1 software to construct a target network diagram of active constituents of Danbie Capsules anti-endometriosis. Then we used the “Network Analyzer” function to analyze the topological attributes of the network, calculating the three network topology parameters: degree of freedom (DOF), closeness centrality (CC), and betweenness centrality (BC) and analyzing the critical active substances of Danbie Capsules in endometriosis treatment according to the parameters.

## Construct an Association Network

The targets of the active substances in Danbie Capsules, known for their anti-endometriosis properties, were queried in the STRING database (<https://string-db.org/>). The search was limited to the species “Homo sapiens” to obtain protein-protein interaction relationships. Cytoscape version 3.9.1 software was employed to visualize the target protein-protein interaction network diagram. The “Network Analyzer” plug-in was utilized to analyze and calculate the metrics of each network node, including DOF, CC, and BC. The targets where all three indexes were above the average value were regarded as the critical targets of anti-endometriosis of Danbie Capsules’ active substances.

## GO Function and KEGG Pathway Enrichment Analysis of the Critical Targets

The Metascape cloud platform (<https://metascape.org/>) was adopted to analyze the function of Gene Ontology (GO) and the enrichment of Kyoto Encyclopedia of Genes and Genomes (KEGGs) on the critical targets of Danbie Capsules in anti-endometriosis treatment, and the analysis results were visualized by Weishenxin cloud platform.

## Molecular Docking Validation of the Critical Active Substances and the Critical Targets of Anti-Endometriosis

The three-dimensional molecular structure formula of critical active substances was obtained from TCMSP and saved as a Mol2 format file. The anti-endometriosis target proteins of the critical active substances of Danbie Capsules were retrieved in the PDB database (<http://www.rcsb.org/>). The water molecules, phosphate, and excess non-active ligands in the proteins were eliminated with the aid of PyMOL software. The treated target proteins were imported into AutoDock Tools software for hydrogenation, charge adding and torsion bonds setting. Then, the critical active substances and target proteins were converted into PDBQT format using AutoDock Tools and set as receptors and ligands respectively. The docking box was fine-tuned with AutoDock Tools to encompass all the protein structures. At the same time, set receptor protein as rigid docking. Run autogrid4 and autodock4 to get docking results, and then got the binding energy. Then used PyMol software to generate a local map of molecular docking.

## Immunohistochemical Method to Verify the Core Differential Genes of Endometriosis - TP53, AKT1

### Samples

Samples were collected from normal endometrium and ectopic endometrium in the rectum of patients in the Sixth Affiliated Hospital of Sun Yat-Sen University for recent 3 years. Six normal endometrial specimens were set as the control group, and 6 ectopic endometrial specimens in the rectum were set as the experimental group.

### Semiquantitative Analysis of TP53 and AKT1 Using Immunohistochemistry

The tissues were made into glass slides with the following steps. Firstly, the slides were baked at 60 °C for 2 h. Next, dewaxing was performed with xylene for 15 min, with the process repeated three times. Then, these tissues were dehydrated with anhydrous, 95%, 90%, 80%, 70% ethanol, and distilled water for 5 min each. Subsequently, the slides were washed with phosphate-buffered saline (PBS) for 5 min, repeating this washing step three times. To repair the tissues, a boiling water bath containing citrate buffer was used for 15 min, followed by natural cooling to room temperature. The slides were washed with PBS for 5 min, repeating this step three times. For further processing, the slides were blocked with 3% hydrogen peroxide for 20 min, followed by washing with PBS for 5 min, repeating this step three times. Subsequently, the slides were blocked with normal fetal bovine serum at 37 °C for 20 min. Next, the primary

antibody was incubated at 4 °C overnight, followed by rewarming for 20 min after overnight, washing with PBS for 5 min, and repeating this washing step three times. The slides were then incubated with the secondary antibody incubation, at 37 °C for 20 min, followed by washing with PBS for 5 min, repeating this washing step three times. To visualize the results, the DAB was used for color development, the slides were observed under the microscope, and the reaction was terminated in time. Counterstaining was performed with hematoxylin for 5 min, followed by rinsing with tap water. Differentiation was carried out with 1% hydrochloric acid alcohol (75%) solution for 30s, followed by rinsing with tap water for 5 min, and bluing. To prepare the slides for preparation, they were dehydrated with 70%, 80%, 90%, 95%, and anhydrous ethanol for 5 min each, and xylene for 15 min, repeating three times. A layer of neutral gum was applied to seal the slides. Finally, these gray values of the protein bands on the slides were analyzed using Image J software for further analysis.

## Results

### Collection and Target Screening of the Active Substances in Danbie Capsules

In literature data and the TCMSP database, Danbie Capsules contained 2120 kinds of active substances, including 55 Largehead Atractylodes Rhizome, 94 Scutellaria Barbata, 125 Radix Angelicae Sinensis, 202 Herba Scutellariae Barbatae, 147 Eucommia ulmoides Oliv., 81 Radix Curcumae, 220 Ramulus Cinnamomi, 20 Seaweed, 975 Rhizoma Sparganii, 119 Radix Notoginseng, 66 Semen Persicae, and 16 Turtle Carapace. Then, 183 active substances were obtained under the conditions of DL  $\geq$  0.18 and OB  $\geq$  30%, including 7 from Largehead Atractylodes Rhizome, 29 from Scutellaria Barbata, 2 from Radix Angelicae Sinensis, 65 from Herba Scutellariae Barbatae, 28 from Cortex Eucommiae, 3 from Radix Curcumae, 7 from Ramulus Cinnamomi, 4 from Seaweed, 5 from Rhizoma Sparganii, 8 from Radix Notoginseng, 23 Semen Persicae, and

**Table 1** The Active Substances in Danbie Capsules

Drug	MOL_ID	Molecule_Name	OB	DL
Baizhu	MOL000020	12-senecioid-2E,8E,10E-atractylentriol	62.39646702	0.22294
Baizhu	MOL000021	14-acetyl-12-senecioid-2E,8E,10E-atractylentriol	60.3128707	0.30534
Baizhu	MOL000022	14-acetyl-12-senecioid-2E,8Z,10E-atractylentriol	63.37091823	0.29956
Baizhu	MOL000028	$\alpha$ -Amyrin	39.51208978	0.7629
Baizhu	MOL000033	(3S,8S,9S,10R,13R,14S,17R)-10,13-dimethyl-17-[(2R,5S)-5-propan-2-yl-octan-2-yl]-2,3,4,7,8,9,11,12,14,15,16,17-dodecahydro-1H-cyclopenta[a]phenanthren-3-ol	36.22847056	0.78288
Baizhu	MOL000049	3 $\beta$ -acetoxyatractylone	54.06671707	0.21906
Baizhu	MOL000072	8 $\beta$ -ethoxy atractylenolide III	35.95091928	0.21079
Banzhilian	MOL001040	(2R)-5,7-dihydroxy-2-(4-hydroxyphenyl)chroman-4-one	42.36332114	0.21141
Banzhilian	MOL012245	5,7,4'-trihydroxy-6-methoxyflavanone	36.62688628	0.26833
Banzhilian	MOL012246	5,7,4'-trihydroxy-8-methoxyflavanone	74.23522001	0.26479
Banzhilian	MOL012248	5-hydroxy-7,8-dimethoxy-2-(4-methoxyphenyl)chromone	65.81880606	0.32874
Banzhilian	MOL012250	7-hydroxy-5,8-dimethoxy-2-phenyl-chromone	43.7169646	0.25376
Banzhilian	MOL012251	Chrysin-5-methylether	37.2683358	0.20317
Banzhilian	MOL012252	9,19-cyclolanost-24-en-3-ol	38.68565906	0.78074
Banzhilian	MOL002776	Baicalin	40.12360996	0.75264
Banzhilian	MOL012254	Campesterol	37.57681789	0.71486
Banzhilian	MOL000953	CLR	37.87389754	0.67677
Banzhilian	MOL000358	Beta-sitosterol	36.91390583	0.75123
Banzhilian	MOL012266	Rivularin	37.94023355	0.3663
Banzhilian	MOL001973	Sitosterol acetate	40.38964165	0.85102
Banzhilian	MOL012269	Stigmasta-5,22-dien-3-ol-acetate	46.44190225	0.85814
Banzhilian	MOL012270	Stigmastan-3,5,22-triene	45.02668769	0.71047
Banzhilian	MOL000449	Stigmasterol	43.82985158	0.75665
Banzhilian	MOL000173	Wogonin	30.68456706	0.22942

(Continued)

Table 1 (Continued).

Drug	MOL_ID	Molecule_Name	OB	DL
Banzhilian	MOL001735	Dinatin	30.97205344	0.27025
Banzhilian	MOL001755	24-Ethylcholest-4-en-3-one	36.08361164	0.75703
Banzhilian	MOL002714	Baicalein	33.51891869	0.20888
Banzhilian	MOL002719	6-Hydroxynaringenin	33.22920875	0.24203
Banzhilian	MOL002915	Salvigenin	49.06592606	0.33279
Banzhilian	MOL000351	Rhamnazin	47.14113124	0.33648
Banzhilian	MOL000359	Sitosterol	36.91390583	0.7512
Banzhilian	MOL005190	Eriodictyol	71.7926526	0.24372
Banzhilian	MOL005869	Daucostero_qt	36.91390583	0.75177
Banzhilian	MOL000006	Luteolin	36.16262934	0.24552
Banzhilian	MOL008206	Moslosooflavone	44.08795959	0.25331
Banzhilian	MOL000098	Quercetin	46.43334812	0.27525
Danggui	MOL000358	Beta-sitosterol	36.91390583	0.75123
Danggui	MOL000449	Stigmasterol	43.82985158	0.75665
Danshen	MOL001601	1,2,5,6-tetrahydrotanshinone	38.74538672	0.35791
Danshen	MOL001659	Poriferasterol	43.82985158	0.75596
Danshen	MOL001771	Poriferast-5-en-3beta-ol	36.91390583	0.75034
Danshen	MOL001942	Isoimperatorin	45.46424674	0.22524
Danshen	MOL002222	Sugiol	36.11353486	0.27648
Danshen	MOL002651	Dehydrotanshinone II A	43.76228599	0.40019
Danshen	MOL002776	Baicalin	40.12360996	0.75264
Danshen	MOL000569	Digallate	61.84861803	0.25635
Danshen	MOL000006	Luteolin	36.16262934	0.24552
Danshen	MOL006824	$\alpha$ -amyrin	39.51208978	0.76221
Danshen	MOL007036	5,6-dihydroxy-7-isopropyl-1,1-dimethyl-2,3-dihydrophenanthren-4-one	33.76525236	0.28585
Danshen	MOL007041	2-isopropyl-8-methylphenanthrene-3,4-dione	40.86015408	0.22897
Danshen	MOL007045	3 $\alpha$ -hydroxytanshinonella	44.92933597	0.44272
Danshen	MOL007048	(E)-3-[2-(3,4-dihydroxyphenyl)-7-hydroxy-benzofuran-4-yl]acrylic acid	48.24363244	0.31229
Danshen	MOL007049	4-methylenemiltirone	34.34867589	0.22726
Danshen	MOL007050	2-(4-hydroxy-3-methoxyphenyl)-5-(3-hydroxypropyl)-7-methoxy-3-benzofurancarboxaldehyde	62.78414726	0.39628
Danshen	MOL007051	6-o-syringyl-8-o-acetyl shanzhiside methyl ester	46.6906586	0.71145
Danshen	MOL007058	Formyltanshinone	73.444622	0.41736
Danshen	MOL007059	3-beta-Hydroxymethylenetanshinone	32.16103376	0.40894
Danshen	MOL007061	Methylenetanshinone	37.07319368	0.36017
Danshen	MOL007063	Przewalskin a	37.10650066	0.64901
Danshen	MOL007064	Przewalskin b	110.3240001	0.43809
Danshen	MOL007068	Przewaquinone B	62.24005962	0.41374
Danshen	MOL007069	Przewaquinone c	55.7416731	0.40408
Danshen	MOL007070	(6S,7R)-6,7-dihydroxy-1,6-dimethyl-8,9-dihydro-7H-naphtho[8,7-g]benzofuran-10,11-dione	41.31045706	0.453
Danshen	MOL007071	Przewaquinone f	40.30788399	0.45925
Danshen	MOL007077	Sclareol	43.67068458	0.2058
Danshen	MOL007079	Tanshinaldehyde	52.4747043	0.45196
Danshen	MOL007081	Danshenol B	57.9508753	0.55764
Danshen	MOL007082	Danshenol A	56.96524899	0.52172
Danshen	MOL007085	Salvilenone	30.38365387	0.37639
Danshen	MOL007088	Cryptotanshinone	52.34196226	0.39555
Danshen	MOL007093	Dan-shexinkum d	38.88302101	0.55453
Danshen	MOL007094	Danshenspiroketallactone	50.43128103	0.3067
Danshen	MOL007098	Deoxyneocryptotanshinone	49.40034705	0.28555

(Continued)

Table I (Continued).

Drug	MOL_ID	Molecule_Name	OB	DL
Danshen	MOL007100	Dihydrotanshinlactone	38.6847683	0.32227
Danshen	MOL007101	Dihydrotanshinone I	45.04327919	0.36015
Danshen	MOL007105	Epidanshenspiroketallactone	68.27315929	0.30549
Danshen	MOL007107	C09092	36.06948986	0.2474
Danshen	MOL007108	Isocryptotanshinone	54.98193246	0.39449
Danshen	MOL007111	Isotanshinone II	49.91602574	0.39674
Danshen	MOL007115	Manool	45.04431636	0.20208
Danshen	MOL007118	Microstegiol	39.61229457	0.27734
Danshen	MOL007119	Miltionone I	49.68439433	0.32125
Danshen	MOL007120	Miltionone II	71.02970321	0.43711
Danshen	MOL007121	Miltipolone	36.55611206	0.36803
Danshen	MOL007122	Miltirone	38.75698635	0.25418
Danshen	MOL007123	Miltirone II	44.95106648	0.23537
Danshen	MOL007124	Neocryptotanshinone II	39.46299114	0.23157
Danshen	MOL007125	Neocryptotanshinone	52.48799701	0.32306
Danshen	MOL007127	1-methyl-8,9-dihydro-7H-naphtho[5,6-g]benzofuran-6,10,11-trione	34.72082213	0.36634
Danshen	MOL007130	Prolithospermic acid	64.37096207	0.31017
Danshen	MOL007132	(2R)-3-(3,4-dihydroxyphenyl)-2-[(Z)-3-(3,4-dihydroxyphenyl)acryloyl]oxy-propionic acid	109.3805241	0.35119
Danshen	MOL007140	(Z)-3-[2-[(E)-2-(3,4-dihydroxyphenyl)vinyl]-3,4-dihydroxy-phenyl]acrylic acid	88.53602101	0.25869
Danshen	MOL007141	Salvianolic acid g	45.56485578	0.60602
Danshen	MOL007142	Salvianolic acid j	43.37604991	0.72497
Danshen	MOL007143	Salvilenone I	32.43470856	0.22895
Danshen	MOL007145	Salviolone	31.72415039	0.23568
Danshen	MOL007149	NSC 122421	34.49292309	0.27645
Danshen	MOL007150	(6S)-6-hydroxy-1-methyl-6-methylol-8,9-dihydro-7H-naphtho[8,7-g]benzofuran-10,11-quinone	75.38587847	0.4551
Danshen	MOL007151	Tanshindiol B	42.66581049	0.45303
Danshen	MOL007152	Przewaquinone E	42.85485204	0.45301
Danshen	MOL007154	Tanshinone iia	49.88730004	0.39781
Danshen	MOL007155	(6S)-6-(hydroxymethyl)-1,6-dimethyl-8,9-dihydro-7H-naphtho[8,7-g]benzofuran-10,11-dione	65.25893771	0.44871
Danshen	MOL007156	Tanshinone VI	45.63730602	0.29549
Duzhong	MOL002058	40,957-99-I	57.20447445	0.61872
Duzhong	MOL000211	Mairin	55.37707338	0.7761
Duzhong	MOL000358	Beta-sitosterol	36.91390583	0.75123
Duzhong	MOL000422	Kaempferol	41.88224954	0.24066
Duzhong	MOL004367	Olivil	62.22859563	0.40642
Duzhong	MOL000443	Erythraline	49.17676997	0.55031
Duzhong	MOL005922	Acanthoside B	43.35308428	0.76689
Duzhong	MOL006709	AIDS214634	92.42724327	0.54906
Duzhong	MOL007059	3-beta-Hydroxymethylenetanshinone	32.16103376	0.40894
Duzhong	MOL000073	Ent-Epicatchin	48.95984114	0.24162
Duzhong	MOL007563	Yangambin	57.52544673	0.80801
Duzhong	MOL009007	Eucommin A	30.51335769	0.84815
Duzhong	MOL009009	(+)-medioresinol	87.18865939	0.61875
Duzhong	MOL009015	(-)-Tabernemontanine	58.66917753	0.60719
Duzhong	MOL009027	Cyclopamine	55.42172002	0.82136
Duzhong	MOL009029	Dehydronicoferyl alcohol 4, gamma'-di-O-beta-D-glucopyranoside_qt	51.44225525	0.39505
Duzhong	MOL009030	Dehydriedugenol	30.10301535	0.23906
Duzhong	MOL009031	Cinchonan-9-al, 6'-methoxy-, (9R)-	68.2150183	0.40098

(Continued)

Table 1 (Continued).

Drug	MOL_ID	Molecule_Name	OB	DL
Duzhong	MOL009038	GBGB	45.57744755	0.82668
Duzhong	MOL009042	Helenalin	77.01051009	0.19049
Duzhong	MOL009047	(+)-Eudesmin	33.28664314	0.62037
Duzhong	MOL009053	4-[(2S,3R)-5-[(E)-3-hydroxyprop-1-enyl]-7-methoxy-3-methylol-2,3-dihydrobenzofuran-2-yl]-2-methoxy-phenol	50.75513649	0.3948
Duzhong	MOL009055	Hirsutin_qt	49.81498455	0.37152
Duzhong	MOL009057	Liriodendrin_qt	53.13736321	0.79961
Duzhong	MOL000098	Quercetin	46.43334812	0.27525
Duzhong	MOL002773	Beta-carotene	37.18433337	0.58358
Duzhong	MOL008240	(E)-3-[4-[(1R,2R)-2-hydroxy-2-(4-hydroxy-3-methoxy-phenyl)-1-methylol-ethoxy]-3-methoxy-phenyl]acrolein	56.31706329	0.36095
Duzhong	MOL011604	Syringetin	36.82222268	0.37414
Ezhu	MOL000296	Hederagenin	36.91390583	0.75072
Ezhu	MOL000906	Wenjine	47.92807652	0.272
Ezhu	MOL000940	Bisdemethoxycurcumin	77.38200887	0.26088
Ezhu	MOL001736	(-)-taxifolin	60.50621692	0.27342
Ezhu	MOL000358	Beta-sitosterol	36.91390583	0.75123
Ezhu	MOL000359	Sitosterol	36.91390583	0.7512
Ezhu	MOL000492	(+)-catechin	54.82643405	0.24164
Ezhu	MOL000073	Ent-Epicatechin	48.95984114	0.24162
Ezhu	MOL004576	Taxifolin	57.84156034	0.27345
Ezhu	MOL011169	Peroxyergosterol	44.39151838	0.82
Haizao	MOL010578	N-[(1S)-1-(benzyl)-2-[[[(1S)-1-(benzyl)-2-hydroxy-ethyl]amino]-2-keto-ethyl]benzamide	45.75831251	0.43303
Haizao	MOL010580	Diglycol dibenzoate	59.21885418	0.27376
Haizao	MOL005440	Isofucosterol	43.77639556	0.7576
Haizao	MOL000098	Quercetin	46.43334812	0.27525
Sanleng	MOL001297	Trans-gondoic acid	30.70294255	0.19744
Sanleng	MOL000296	Hederagenin	36.91390583	0.75072
Sanleng	MOL000358	Beta-sitosterol	36.91390583	0.75123
Sanleng	MOL000392	Formononetin	69.67388061	0.21202
Sanleng	MOL000449	Stigmasterol	43.82985158	0.75665
Sanqi	MOL001494	Mandenol	41.99620045	0.19321
Sanqi	MOL001792	DFV	32.76272375	0.18316
Sanqi	MOL002879	Diop	43.59332547	0.39247
Sanqi	MOL000358	Beta-sitosterol	36.91390583	0.75123
Sanqi	MOL000449	Stigmasterol	43.82985158	0.75665
Sanqi	MOL005344	Ginsenoside rh2	36.31951162	0.55868
Sanqi	MOL007475	Ginsenoside f2	36.43174722	0.25282
Sanqi	MOL000098	Quercetin	46.43334812	0.27525
Taoren	MOL001323	Sitosterol alpha I	43.28127042	0.78354
Taoren	MOL001328	2,3-didehydro GA70	63.29362943	0.49632
Taoren	MOL001329	2,3-didehydro GA77	88.08054638	0.53017
Taoren	MOL001339	GA119	76.36423404	0.49382
Taoren	MOL001340	GA120	84.84963921	0.45279
Taoren	MOL001342	GA121-isolactone	72.69926164	0.5371
Taoren	MOL001343	GA122	64.79328513	0.49617
Taoren	MOL001344	GA122-isolactone	88.11097358	0.5371
Taoren	MOL001348	Gibberellin 17	94.64114807	0.49443
Taoren	MOL001349	4a-formyl-7alpha-hydroxy-1-methyl-8-methylidene-4aalpha,4bbeta-gibbane-1alpha,10beta-dicarboxylic acid	88.59516065	0.46382

(Continued)

**Table 1** (Continued).

Drug	MOL_ID	Molecule_Name	OB	DL
Taoren	MOL001350	GA30	61.71773793	0.54002
Taoren	MOL001351	Gibberellin A44	101.61317	0.54105
Taoren	MOL001352	GA54	64.20664836	0.5349
Taoren	MOL001353	GA60	93.16869233	0.53004
Taoren	MOL001355	GA63	65.54355602	0.53773
Taoren	MOL001358	Gibberellin 7	73.80061824	0.49609
Taoren	MOL001360	GA77	87.89415596	0.52764
Taoren	MOL001361	GA87	68.85254536	0.57188
Taoren	MOL001368	3-O-p-coumaroylquinic acid	37.62790163	0.28636
Taoren	MOL001371	Populoside_qt	108.8854875	0.20476
Taoren	MOL000296	Hederagenin	36.91390583	0.75072
Taoren	MOL000358	Beta-sitosterol	36.91390583	0.75123
Taoren	MOL000493	Campesterol	37.57681789	0.71476
Biejia	MOL005030	11-eicosenoic acid	30.7	0.2
Biejia	MOL010861	Vitamin d	45.66	0.48

2 from Turtle Carapace (Table 1). The DrugBank database was employed to predict the target of screened active substances. In the end, a total of 292 target proteins were obtained.

## Identification of Differential Genes in Endometriosis

By performing a comparative analysis between 6 normal samples and 8 disease samples available in the GEO database, a total of 12,548 differentially expressed genes were identified. Among these genes, 7379 were found to be up-regulated, while 5169 were down-regulated in disease samples compared to the normal samples. There were 559 up-regulated and 586 down-regulated genes after adjusting for  $P$ -value  $< 0.005$  and  $|\log_2(FC)| > 1$ . As could be seen from the map of the gene volcano (Figure 1), in the disease samples, the distribution of differential genes followed a normal distribution pattern, and there was a higher number of significantly down-regulated genes compared to significantly up-regulated genes. The top 20 genes exhibiting the most significant up-regulation and down-regulation are in Figure 2.

## Determination of Targets and Network Construction of Danbie Capsules in Endometriosis Treatment

As shown in Figure 3, there were a total of 24 intersection genes. The regulatory network of the TCM visually demonstrates the targeting relationship between the active substances of Danbie Capsules and the intersection of genes, providing insights into how these compounds interact and influence gene regulation.

Figure 4 illustrates the network diagram of active substances of 11 TCMs in Danbie Capsules (without the involvement of Turtle Carapace) acting on 24 targets, including 60 nodes and 107 edges, showing the multi-component and broad-spectrum targeting action mechanism of Danbie Capsules. In the network diagram, the mean DOF of active substances was 4.28, the average of BC was  $3.27 \times 10^{-2}$  and the average of CC is  $3.27 \times 10^{-2}$ . Among them, the active substances whose topology parameters exceeded the average value were: quercetin,  $\beta$ -sitosterol, and luteolin, suggesting that these ingredients might be the critical active substances of Danbie Capsules in anti-endometriosis.

## PPI Network Construction

The PPI network was shown in Figure 5, with a total of 22 nodes (target proteins PTGER3 and ADH1B were not involved in the interaction) and 214 interaction lines. The darker the color and larger the area of the circular nodes, the higher their DOF and importance. The mean DOF was 19.45, the mean BC was  $2.90 \times 10^{-2}$  and the mean CC was  $6.54 \times 10^{-1}$ . All seven targets exhibited DOM, CC, and BC values that exceeded the mean value, and they were considered the critical targets of Danbie Capsules in anti-endometriosis. The results were shown in Table 2.

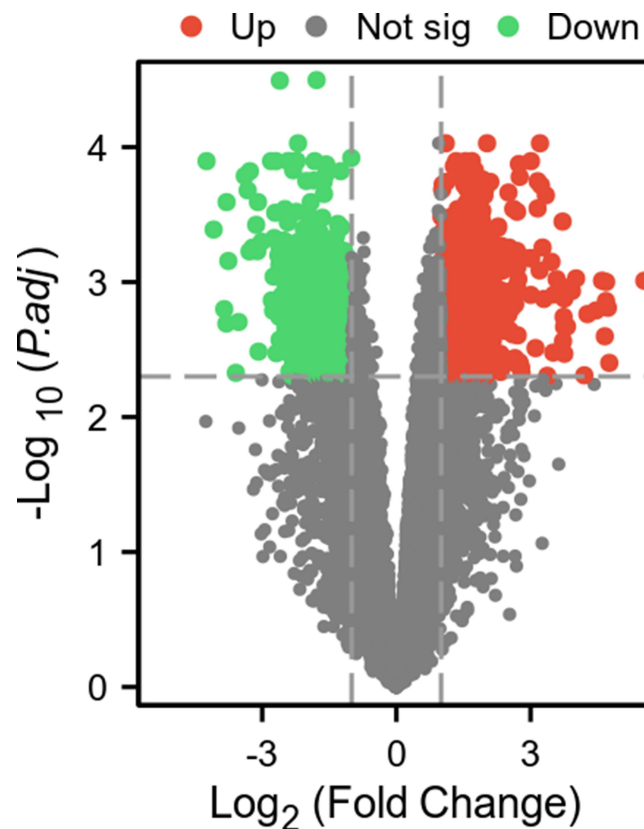


**Figure 1** The map of the gene volcano highlights how genes are distributed across these disease samples. Green and red respectively highlight the up-regulated genes ( $\log_{2}FC > 0$ ) and down-regulated genes ( $\log_{2}FC < 0$ ), while gray highlights the absence of significant differences.

## Analysis of the GO Function and KEGG Pathway Enrichment of the Critical Targets

GO enrichment analysis provides insights into the functional roles of genes at three distinct levels: biological process (BP), cellular component (CC), and molecular function (MF) (Figure 6). BP primarily encompasses the gene's participation in hormone response, cellular reactions to organonitrogen compounds, and cellular responses to nitrogen compounds. CC was mainly related to transcriptional regulator complexes, RNA polymerase II transcriptional regulatory complexes, and glutamatergic synapses. As for the MF level, the gene predominantly engages in interactions such as binding to ubiquitin-protein ligases, binding to kinases, and binding to ubiquitin-like protein ligases. Based on the KEGG enrichment analysis, the therapeutic mechanism of Danbei Capsules in endometriosis primarily revolves around the modulation of human T-cell leukemia virus 1, hepatitis B, and cancer pathways (Figure 7).

Among the identified pathways, the genes, BAX, AKT1, CDKN1, and TTP53, were found to be associated with the highest number of pathways (Figure 8).

## Molecular Docking of Critical Ingredients of Danbei Capsules and Critical Targets of Anti-Endometriosis

The critical active substance luteolin was used for molecular docking with the critical targets TTP53 and AKT1. The affinity between the two target proteins and luteolin was  $< -5$  kcal/mol and the amino acid residues docking with luteolin were shown in Figure 9.

## Immunohistochemical Validation Results

TP53 group: The positive rate of TP53 protein expression in both the control group and the experimental group was 100% (both were highly positive); AKT1 group: The positive rate of AKT1 protein expression in the control group was

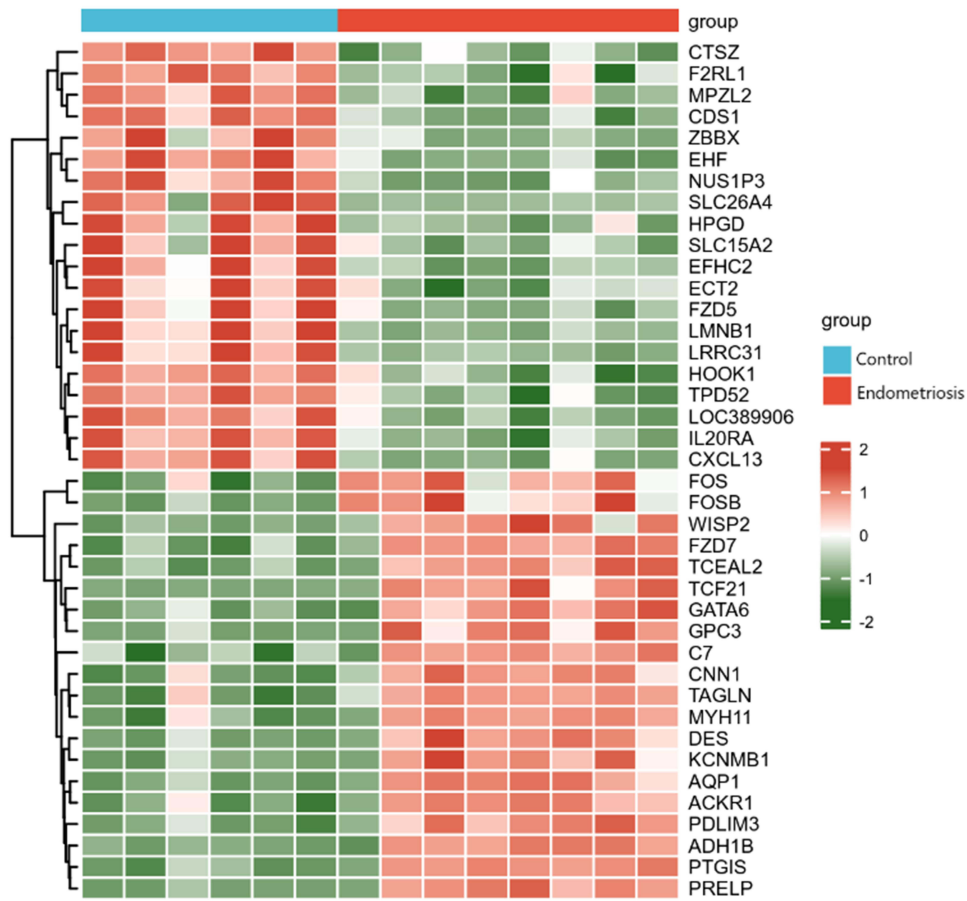


**Figure 2** Map of gene heat. Green and red respectively highlight the genes that are up-regulated ( $\log_{2}FC > 0$ ) and down-regulated ( $\log_{2}FC < 0$ ), while white highlights the absence of significant differences. The first 6 samples were from healthy volunteers; the last 8 samples were from endometriosis patients.

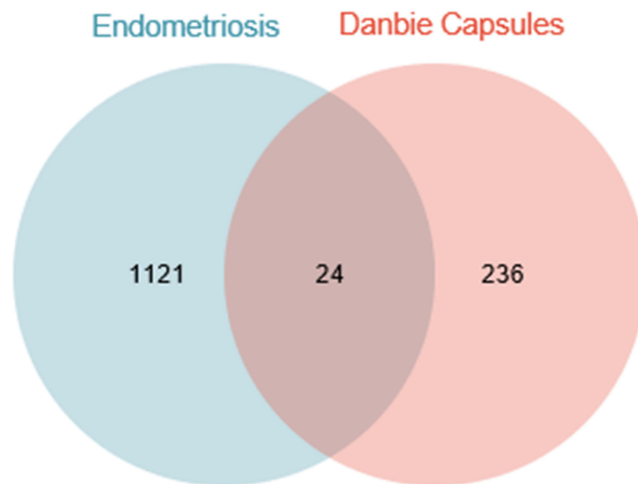


**Figure 3** Venn diagram of targets of Danbie Capsules in endometriosis treatment.

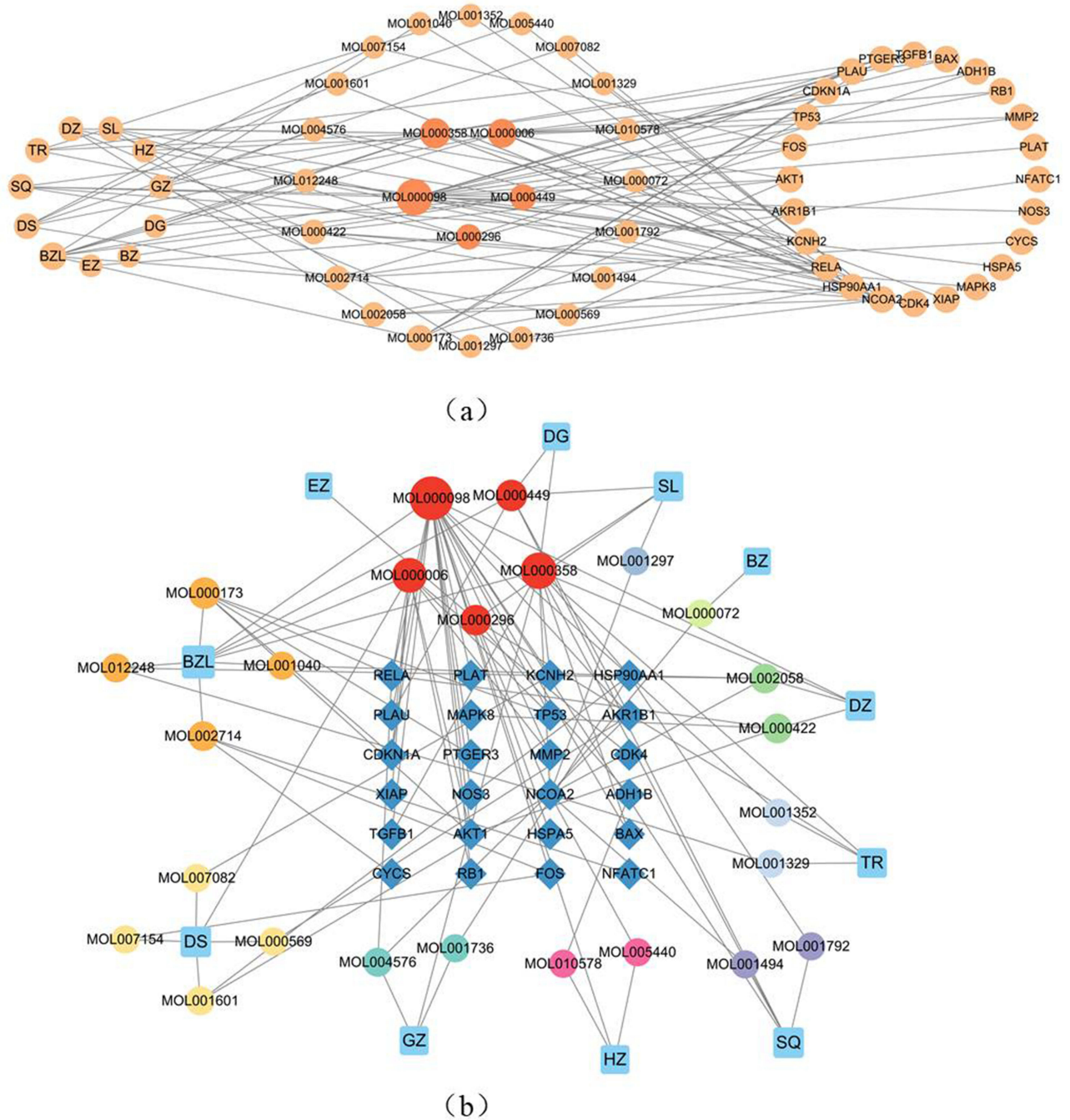


**Figure 4 (a and b)** TCM - Compound - Gene network: The network indicates the interplay and targeting relationship between active substances derived from TCMs and the intersection genes. The Dark colored circles in the middle represent the common components. (b) TCM - Compound - Gene network: The network indicates the interplay and targeting relationship between active substances derived from TCMs and the intersection genes. The blue rectangles indicate the components of Danbie Capsules, the red circles represent the common components, other colorful circles represent the active substances corresponding to each component of Danbie Capsules, and the dark blue diamonds represent the intersection of genes.

83.33% (5 low positive, 1 negative), while the positive rate of AKT1 protein expression in the experimental group was 100% (5 positive, 1 high positive). As shown in Figure 10.

## Discussion

To further study the active substances and targets of Danbie Capsules in the Endometriosis therapy TCMSP and published kinds of literature screened and obtained 183 active substances of Danbie Capsules, combined and intersected

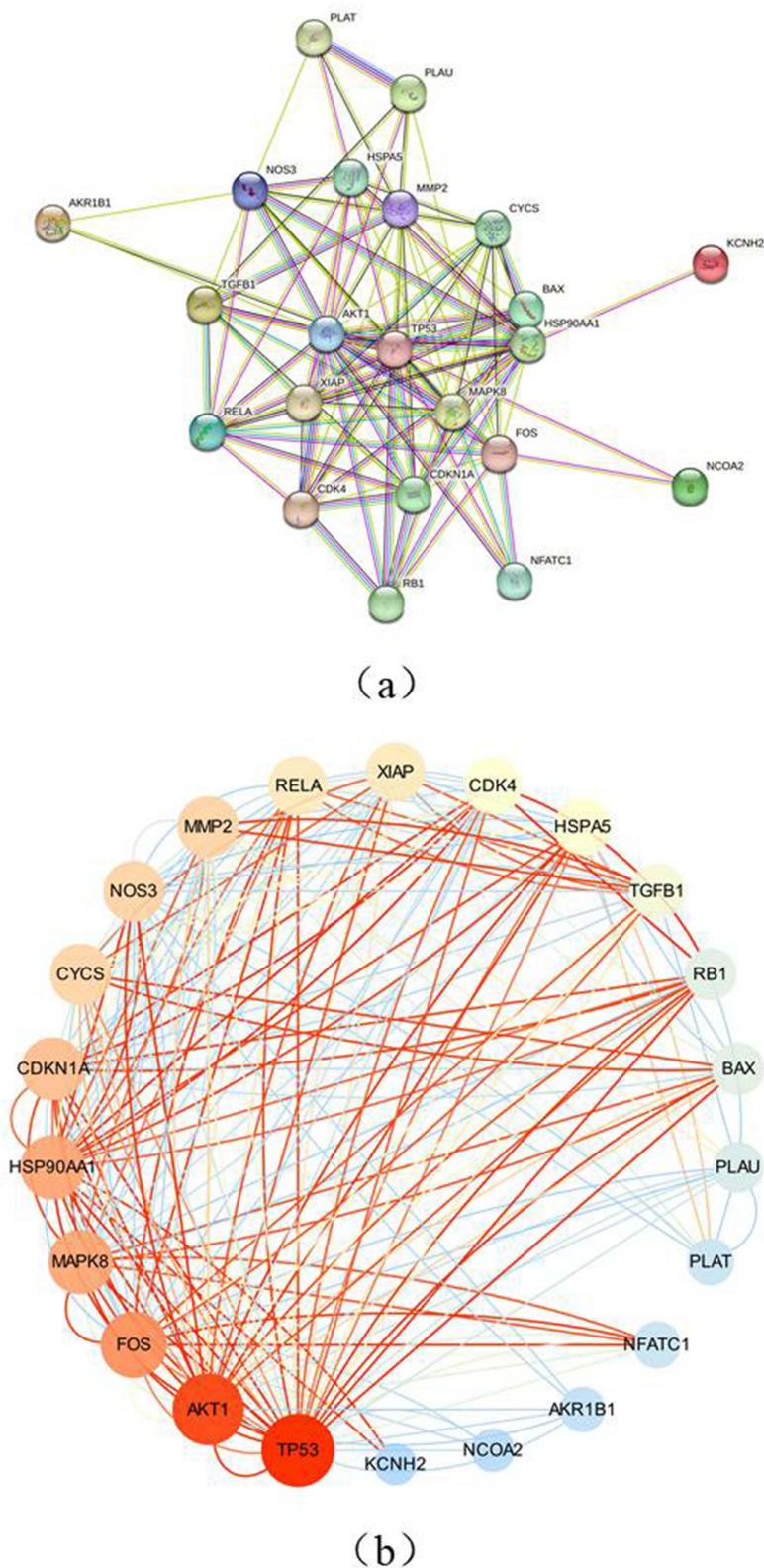


**Figure 5** (a and b) PPI network from the STRING database; b: PPI network: The network shows the protein-protein interaction relationships of 22 target genes, and the darker the color and larger the area of the circular nodes, the higher their DOF.

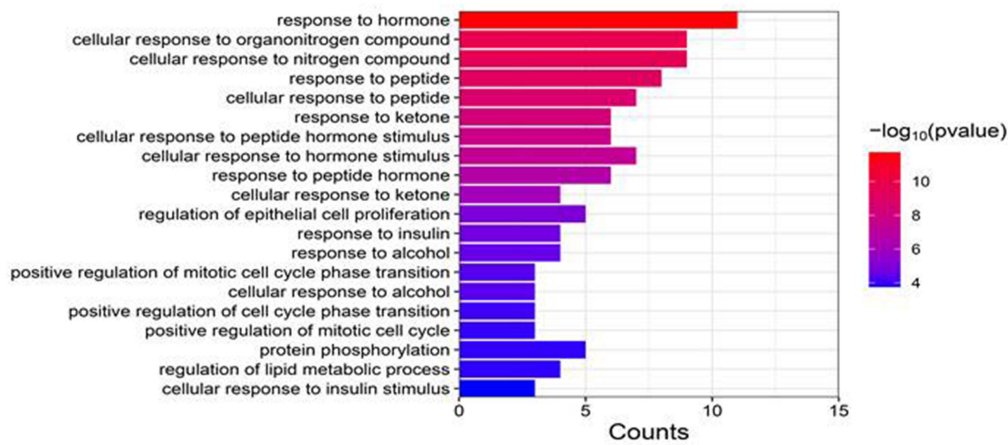
**Table 2** Intersection Genes (Sorted by DOF)

Gene Name	Degree	Betweenness Centrality	Closeness Centrality
TTP53	38	0.149267812	0.913043478
AKT1	36	0.094165772	0.875
FOS	30	0.071929128	0.777777778
HSP90AA1	28	0.108127163	0.75
MAPK8	28	0.032446891	0.75
NOS3	24	0.043091757	0.7
MMP2	24	0.03843428	0.7
CDKN1A	26	0.017419939	0.724137931
CYCS	24	0.011324641	0.7
XIAP	22	0.010736961	0.677419355
RELA	22	0.00829743	0.677419355
CDK4	20	0.005214723	0.65625
HSPA5	20	0.027516112	0.65625
TGFB1	18	0.007301587	0.617647059
RBI	14	4.76E-04	0.583333333
BAX	14	5.95E-04	0.583333333
PLAU	12	0.008688388	0.567567568
NFATC1	8	0	0.525
PLAT	8	0.003061224	0.5
AKR1B1	6	0	0.525
NCOA2	4	0	0.5
KCNH2	2	0	0.4375

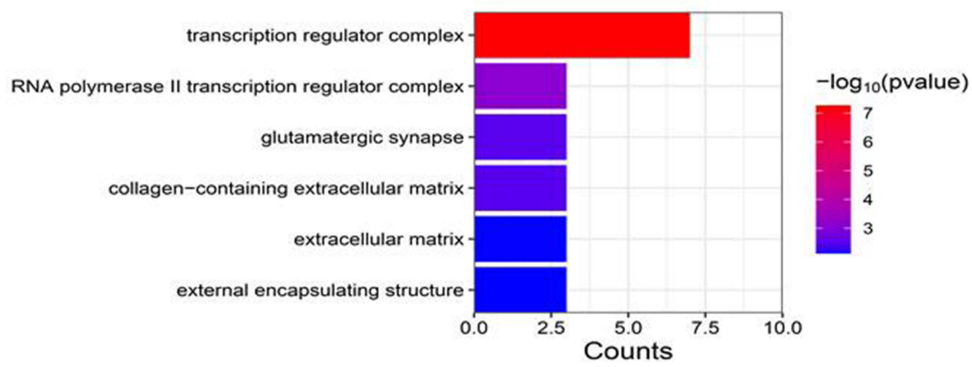
**Note:** The genes highlighted in red are the core genes ranked at the top.

with Endometriosis target genes collected and screened in the GEO database, obtained 24 target genes for Endometriosis treatment, and mapped the target network map of Danbie Capsules active substances against Endometriosis. With the help of Cytoscape version 3.9.1 to analyze this network, the research results obtained Quercetin  $\beta$ -3 critical active substances, sitosterol, and Luteolin. Quercetin and Luteolin are common Flavonoid in nature. They exhibit antioxidant, anti-inflammatory, and anti-tumor effects. Quercetin is widely acknowledged for its exceptional ability to scavenge reactive oxygen species (ROS) efficiently. It also acts as a potent inhibitor of several proinflammatory reactions, including the suppression of tumor necrosis factor-alpha (TNF- $\alpha$ ) and nitric oxide (NO) production. The anti-tumor effects of Quercetin include promoting the loss of cell activity, apoptosis, and apoptosis. Autophagy is achieved by regulating PI3K/Akt/mTOR, Wnt/- catenin, and MAPK/ERK1/2 pathways. Its role in cancer metabolism can target molecular pathways involved in glucose metabolism and mitochondrial function.<sup>7</sup> Luteolin mediated targeting of protein network and microRNAs in different cancers: Focus on JAK-STAT, NOTCH, mTOR, and TRAIL-mediated signaling pathways.<sup>8</sup> As a well-known plant-derived nutrient with anticancer properties,  $\beta$ -sitosterol can help fight against a wide range of cancers, such as breast, stomach, colon, lung, prostate, and leukemia. Extensive research has proven that  $\beta$ -sitosterol can modulate numerous critical cell signaling pathways. It can exert influences on cellular processes such as cell cycle regulation, apoptosis induction, proliferation control, survival promotion, invasion inhibition, angiogenesis suppression, and metastasis prevention. What's more, it also has demonstrated anti-inflammatory, anticancer, hepatoprotective, antioxidant, cardioprotective, and anti-diabetic properties during pharmacological screening without inducing severe toxicity.<sup>9</sup>

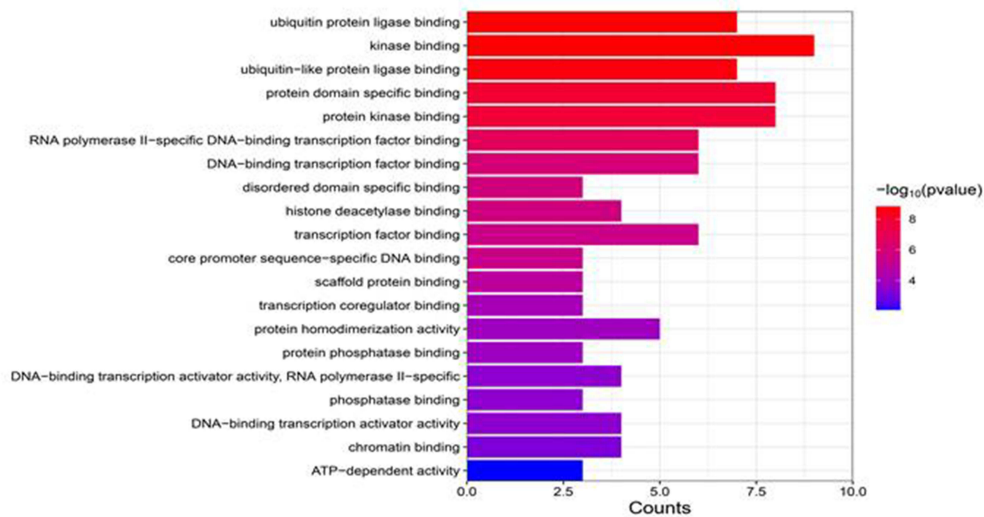
Based on the STRING data analysis platform, PPI network analysis was conducted on 24 anti-endometriosis targets of Danbie Capsules, and seven critical targets (TP53, AKT1, FOS, HSP90AA1, MAPK8, NOS3, MMP2) were identified according to network metrics, including TP53 (regulating cell transcription and apoptosis), AKT1 (regulating cell proliferation), FOS (involving in signal transduction, cell proliferation, and differentiation), HSP90AA1 (facilitating the maturation, maintenance, and precise regulation of specific target proteins, ensuring their proper structural integrity and functionality), and MAPK8 (inducing cell proliferation, differentiation, migration, transformation, and programmed



(a) BP



(b) CC



(c) MF

**Figure 6** (a–c) GO enrichment analysis of Danbie Capsules in endometriosis treatment. In the BP (a), CC (b), and MF (c) columns, the horizontal axis indicates the proportion of genes enriched in each item, and the color indicates the enrichment degree based on P-values (log10 conversion).

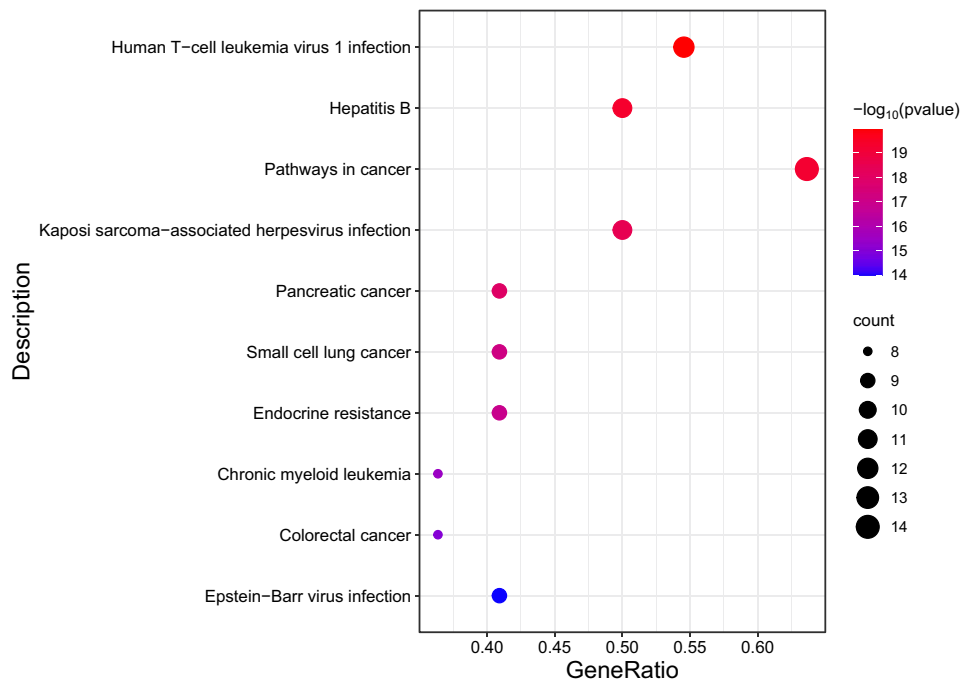


**Figure 7** Bubble chart of KEGG. In the bubble chart of KEGG, the horizontal axis indicates the proportion of genes enriched in each entry, while the vertical axis represents the degree of enrichment based on the P-value (log10 conversion).

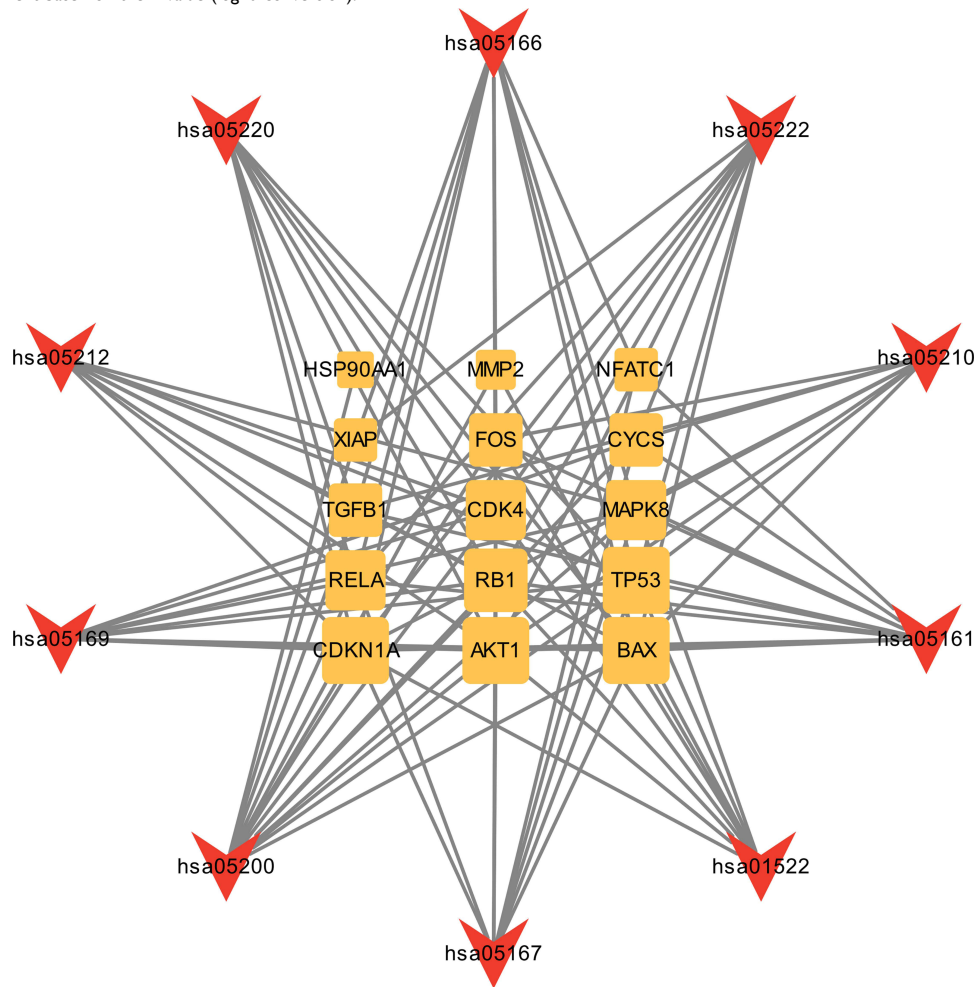


**Figure 8** Danbie Capsules signaling pathway - Anti-endometriosis critical target network.

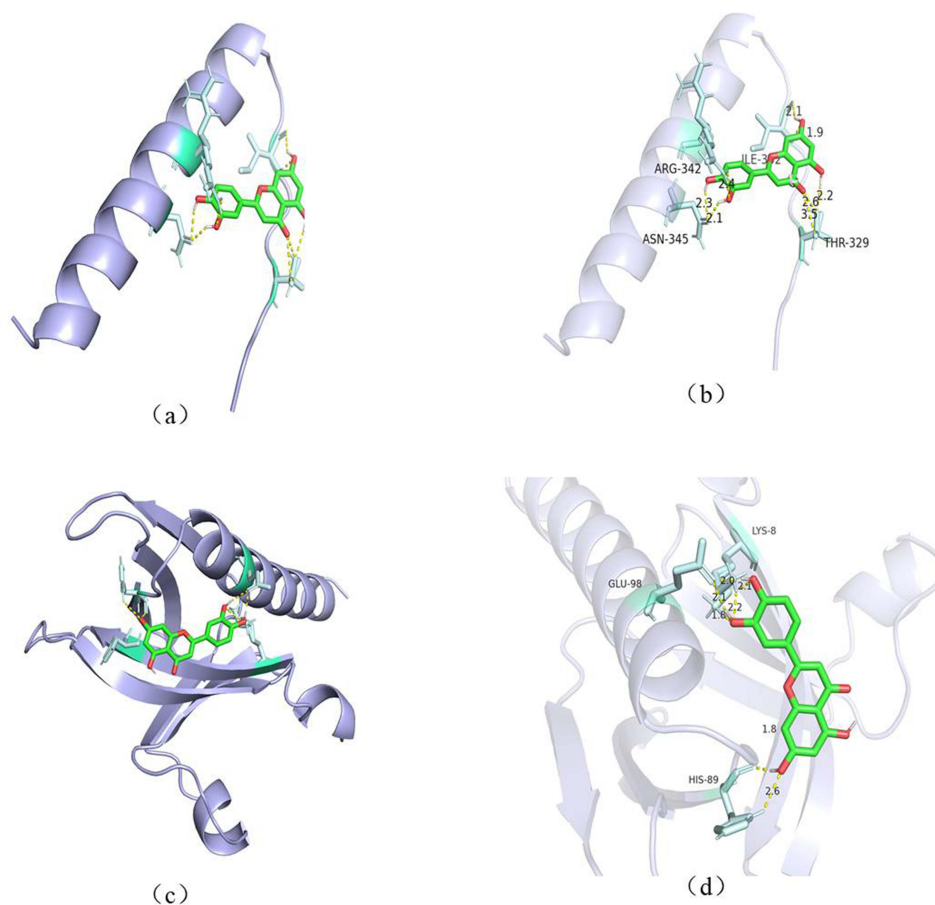


**Figure 9** (a–d), (a and b) Macromolecular docking model of luteolin and TP53; (c and d) Macromolecular docking model of luteolin and AKT1.

cell death). NOS3 is involved in promoting the relaxation of vascular smooth muscle, and MMP2 is involved in extracellular matrix breakdown. The critical component of Luteolin was Macromolecular docking with its two critical targets. In the visualization of the results, it can be seen that there are hydrogen bonding forces and other Intermolecular forces between the small molecule Luteolin and the surrounding amino acid residues, making it stably bound to the active pockets of each protein; The docking results showed that the affinity was less than  $-5\text{kcal/mol}$ , indicating that they were easy to combine and might contribute to the anti-endometriosis effects of Danbie Capsules.

The analysis of GO function and KEGG pathway enrichment of 24 critical targets of the Danbie Capsules against Endometriosis was carried out. The analysis of the GO function enrichment revealed that the Endometriosis therapy with the Danbie Capsules was mainly involved in the response to hormones in vivo, the response of cells to organic nitrogen compounds, and the response of cells to nitrogen compounds. The analysis of the KEGG pathway enrichment revealed that the possible signal pathways of the Danbie Capsules in the Endometriosis therapy were mainly focused on the human T-cell leukemia virus 1 infection pathway, hepatitis B pathway, and cancer pathway. HTLV-1 primarily infects CD4<sup>+</sup> T cells, which are the critical cells in the triggering and establishing of the adaptive immune response.<sup>10</sup> HBV, a hepatotropic virus, has the propensity to induce severe liver diseases, such as acute and chronic hepatitis, cirrhosis, and hepatocellular carcinoma (HCC). Epigenetic alterations, in conjunction with genetic alterations, have long been regarded as the pivotal drivers in the process of carcinogenesis. DNA methylation, histone modifications, and RNA-mediated regulation have been implicated in a multitude of cellular processes critical for the initiation and progression of cancer. A multitude of chromatin-associated and modifying proteins govern these intricate processes, subject to the regulatory influence of signaling pathways. The phosphatidylinositol 3-kinase (PI3K)/AKT pathway (PI3K/AKT) exerts regulatory control over a myriad of biological processes and is commonly dysregulated in human cancers. A growing body of evidence suggests that critical

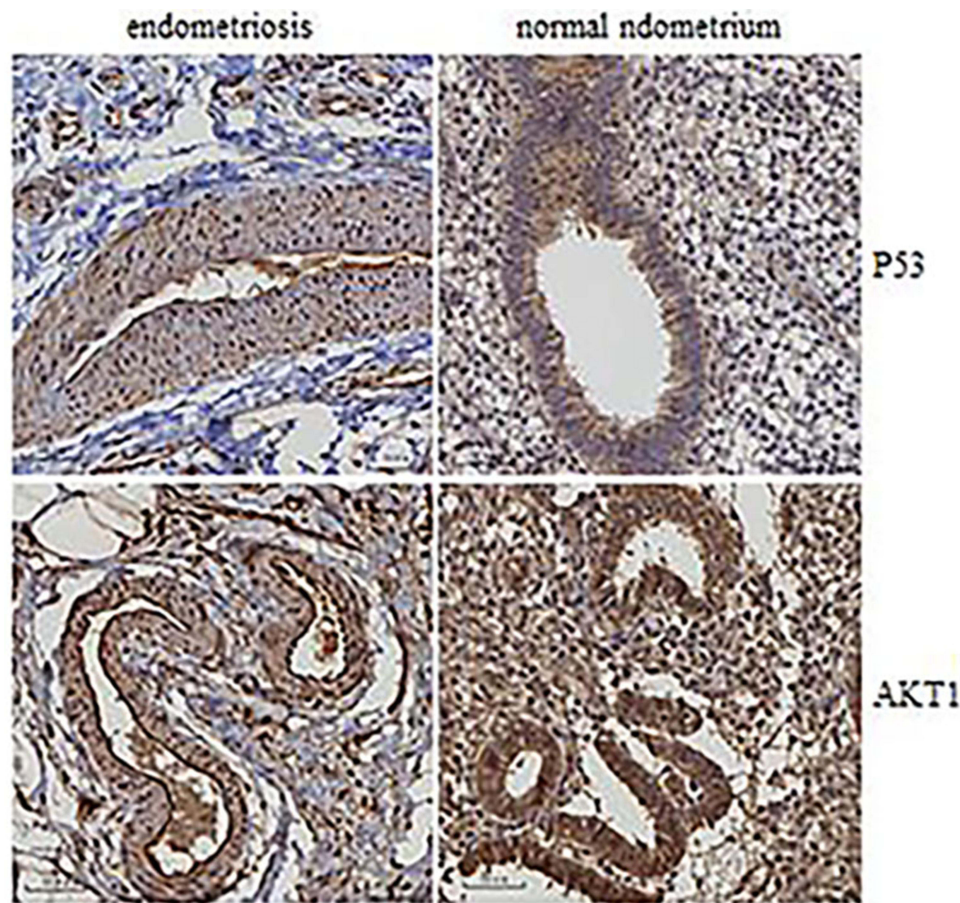


**Figure 10** Expression of P53 and AKT1 in normal endometrium and endometriosis.

epigenetic modifiers are subjected to direct or indirect modulation by PI3K/AKT signaling. Therefore, it contributes to the oncogenicity of the PI3K cascade in cancers.<sup>11</sup> TP53 is the preeminent gene subject to mutations in human cancer, garnering over 100,000 literature citations in PubMed. This pathway holds a prominent position in cancer biology and oncology, tracing its roots back to p53 in 1979. With a myriad of inputs and downstream outputs that contribute to its tumor suppressor role, the p53 pathway constitutes an intricate cellular stress response network.<sup>12</sup> The heterogeneity of KSHV-associated malignancies arises from the interplay of multiple pathophysiologic mechanisms such as chronic antigenic stimulation, immunosuppression, genetic abnormalities, cytokine release and dysregulation, and co-infection with HIV. There is an increasing acknowledgment that inflammatory manifestations in KSHV-associated malignancies (KSHV-MCD, KICS, and KS-IRIS) have been associated with a significant risk of mortality.<sup>13</sup> Pancreatic cancer is believed to be at least partially driven by the presence of somatic mutations in oncogenes and tumor suppressor genes. The most frequently affected genes in PDAC are the oncogene KRAS and the tumor suppressor genes CDKN2A, TP53, and SMAD4.<sup>14</sup> Genomic alterations in small-cell lung cancer include TP53, RB1, TP73, NOTCH, MLL2, MYC, PI3K, BCL2, RICTOR.<sup>15</sup> Insulin resistance is significantly associated with metabolic syndrome, risk-related osteoporosis, and other factors. With the implementation of proper treatment using tyrosine-kinase inhibitors, regular monitoring, and favorable response to therapy, patients suffering from chronic myeloid leukemia can now attain a life expectancy comparable to that of individuals without the disease, offering them a near-normal quality of life.<sup>16</sup>

The lack of research is due to experimental conditions and funding reasons, which led to the selection of immunohistochemical methods for semi-quantitative analysis of the target protein, which cannot be accurately quantified. Therefore, there was no difference in P53 between the two groups, considering the small sample size and limitations of immunohistochemical semi-quantitative methods. Despite these limitations, AKT1 showed some differences between the two groups.

## Conclusion

The active substances of the Danbie Capsules are mainly Quercetin, Luteolin, and  $\beta$ -sitosterol. Seven critical target genes were identified, and two representative genes (TP53 and AKT1) have been verified in Macromolecular docking and immunohistochemical verification. Then we have some insights into the mechanism of the Danbie Capsules in Endometriosis therapy.

## Acknowledgments

There are no conflicts of interest. This study has been approved by the Medical Ethics Committee of the Sixth Affiliated Hospital of Sun Yat-sen University. We confirm that informed consent was obtained from the study participants and the guidelines outlined in the Declaration of Helsinki were followed.

## Disclosure

The authors report no conflicts of interest in this work.

## References

1. Chapron C, Marcellin L, Borghese B, Santulli P. Rethinking mechanisms, diagnosis and management of endometriosis. *Nat Rev Endocrinol.* 2019;15(11):666–682. doi:10.1038/s41574-019-0245-z
2. Mehedintu C, Plotogea MN, Ionescu S, Antonovici M. Endometriosis still a challenge. *J Med Life.* 2014;7(3):349.
3. Hu S, Liu D. Effect of Danbie Capsule on Endometriosis Rats. *Jiangxi J Tradit Chin Med.* 2017;48(02):32–34.
4. Liu Z, Xiong T, Hu Y, Lu Q, Liao X, Liao H. Study on the anti endometriosis mechanism of danbie capsule. *Nei Mongol J Tradit Chin Med.* 2009;28(08):34–35.
5. Zhang C. *Study on Anti Endometriosis Effect and Mechanism of Danbie Capsule.* Master. Guangzhou University of Chinese Medicine; 2008.
6. Wei M, Li H, Li Q, et al. Based on network pharmacology to explore the molecular targets and mechanisms of gegen qinlian decoction for the treatment of ulcerative colitis. *Biomed Res Int.* 2020;2020:1–18. doi:10.1155/2020/5217405
7. Tian Y. Study on the clinical effect and mechanism of huoxue ruanjian fuzheng prescription on hepatic fibrosis after hepatitis B. Master. *Beij Univ Chin Med.* 2021;2021:1.
8. Reyes-Farias M, Carrasco-Pozo C. The anti-cancer effect of quercetin: molecular implications in cancer metabolism. *Int J Mol Sci.* 2019;20:3177. doi:10.3390/ijms20123177
9. Farooqi AA, Butt G, El-Zahaby SA, et al. Luteolin mediated targeting of protein network and microRNAs in different cancers: focus on JAK-STAT, NOTCH, mTOR and TRAIL-mediated signaling pathways. *Pharmacol Res.* 2020;160:105188. doi:10.1016/j.phrs.2020.105188
10. Khan Z, Nath N, Rauf A, et al. Multifunctional roles and pharmacological potential of beta-sitosterol: emerging evidence toward clinical applications. *Chem Biol Interact.* 2022;365:110117. doi:10.1016/j.cbi.2022.110117
11. Forlani G, Shallak M, Accolla RS, Romanelli MG. HTLV-1 infection and pathogenesis: new insights from cellular and animal models. *Int J Mol Sci.* 2021;22(15):8001. doi:10.3390/ijms22158001
12. Yang Q, Jiang W, Hou P. Emerging role of PI3K/AKT in tumor-related epigenetic regulation. *Semin Cancer Biol.* 2019;59:112–124. doi:10.1016/j.semcancer.2019.04.001
13. Hernandez Borrero LJ, El-Deiry WS. Tumor suppressor p53: biology, signaling pathways, and therapeutic targeting. *Biochim Biophys Acta Rev Cancer.* 2021;1876(1):188556. doi:10.1016/j.bbcan.2021.188556
14. Bhutani M, Polizzotto MN, Uldrick TS, Yarchoan R. Kaposi sarcoma-associated herpesvirus-associated malignancies: epidemiology, pathogenesis, and advances in treatment. *Semin Oncol.* 2015;42(2):223–246. doi:10.1053/j.seminoncol.2014.12.027
15. Wood LD, Canto MI, Jaffee EM, Simeone DM. Pancreatic Cancer: pathogenesis, Screening, Diagnosis, and Treatment. *Gastroenterology.* 2022;163(2):386–402 e1. doi:10.1053/j.gastro.2022.03.056
16. Wang Y, Zou S, Zhao Z, Liu P, Ke C, Xu S. New insights into small-cell lung cancer development and therapy. *Cell Biol Int.* 2020;44(8):1564–1576. doi:10.1002/cbin.11359

International Journal of General Medicine

Dovepress

Publish your work in this journal

The International Journal of General Medicine is an international, peer-reviewed open-access journal that focuses on general and internal medicine, pathogenesis, epidemiology, diagnosis, monitoring and treatment protocols. The journal is characterized by the rapid reporting of reviews, original research and clinical studies across all disease areas. The manuscript management system is completely online and includes a very quick and fair peer-review system, which is all easy to use. Visit <http://www.dovepress.com/testimonials.php> to read real quotes from published authors.

Submit your manuscript here: <https://www.dovepress.com/international-journal-of-general-medicine-journal>